



OPEN

DLAT is a promising prognostic marker and therapeutic target for hepatocellular carcinoma: a comprehensive study based on public databases

Peng Zhang^{1,6}, Jiang-Hua Zhao^{2,6}, Liu-Xia Yuan³, Lin-Ling Ju³, Hui-Xuan Wang³, Feng Wang⁴, Lin Chen³✉ & Wei-Hua Cai⁵✉

Cuproptosis is a new mechanism of cell death that differs from previously identified regulatory cell death mechanisms. Cuproptosis induction holds promise as a new tumour treatment. Therefore, we investigated the value of cuproptosis-related genes in the management of hepatocellular carcinoma (HCC). The cuproptosis-related gene Dihydroliipoamide S-Acetyltransferase (DLAT) were significantly upregulated in liver cancer tissues. High levels of DLAT were an independent prognostic factor for shorter overall survival (OS) time. DLAT and its related genes were mainly involved in cell metabolism, tumor progression and immune regulation. DLAT was significantly associated with the level of immune cell infiltration and immune checkpoints in HCC. HCC with high DLAT expression was predicted to be more sensitive to sorafenib treatment. The risk prognostic signature established based on DLAT and its related genes had a good prognostic value. The cuproptosis-related gene DLAT is a promising independent prognostic marker and therapeutic target in HCC. The new prognostic signature can effectively predict the prognosis of HCC patients.

Abbreviations

TCGA	The cancer genome atlas
ACLBI	Assistant for clinical bioinformatics
GDSC	The genomics of drug sensitivity in cancer
CCLL	Cancer cell line encyclopedia
ICGC	International cancer genome consortium
ROC	Receiver operating characteristic

Liver cancer is one of the most common types of cancer worldwide, and its incidence continues to increase every year, making it a global health challenge. By 2025, an estimated 1 million new cases of liver cancer will be diagnosed each year¹. Of these, HCC accounts for 90% of all primary liver cancers and hepatitis virus infection remains a major risk factor for HCC^{2,3}. Currently, the incidence and mortality rate of HCC remain high^{1,4}. Notably the mechanism of occurrence and development of HCC has not been fully elucidated, and various biological mechanisms are involved in its process. At present, immunotherapy and targeted therapy have become good treatment strategies for nonsurgical patients, but they are limited by the lack of effective remission predictors, drug resistance and side effects. Therefore, the search for biomarkers of potential value is important for the early diagnosis of HCC and development of treatment strategies^{5,6}.

¹Nantong Institute of Liver Disease, Department of Hepatobiliary Surgery, Nantong Third People's Hospital, Affiliated Nantong Hospital 3 of Nantong University, Nantong, China. ²Medical School of Nantong University, Nantong Third People's Hospital, Affiliated Nantong Hospital 3 of Nantong University, Nantong, China. ³Nantong Institute of Liver Disease, Nantong Third People's Hospital, Affiliated Nantong Hospital 3 of Nantong University, Nantong, China. ⁴Department of Laboratory Medicine, Affiliated Hospital of Nantong University, Medical School of Nantong University, Nantong, China. ⁵Department of Hepatobiliary Surgery, Nantong Third People's Hospital, Affiliated Nantong Hospital 3 of Nantong University, Nantong, China. ⁶These authors contributed equally: Peng Zhang and Jiang-Hua Zhao. ✉email: xiaobei227@sina.com; cwhntsy@163.com

Cell death is closely related to the occurrence and development of tumors. Current studies have found that known cell death modes such as apoptosis, necroptosis, pyroptosis and ferroptosis, play key roles in tumor formation and progression^{7,8}. In 2022, researchers discovered a new form of cell death, named cuproptosis, and the study was published in *Science*. The essential trace element copper is involved in biological processes, including mitochondrial respiration, as a cofactor, and relatively low intracellular copper concentrations maintain cellular homeostasis⁹. Cuproptosis is a regulated form of cell death triggered by excess intracellular copper and depends on mitochondrial respiration. Excess copper promotes the aggregation of lipid acylated proteins and loss of iron-sulfur cluster proteins by binding to the lipid acylated components of the tricarboxylic acid cycle, leading to protein hydrotoxic stress and ultimately cell death¹⁰. The current study identified cuproptosis-related genes including DLAT, Lipoyltransferase 1 (LIPT1), Lipoic Acid Synthetase (LIAS), Pyruvate Dehydrogenase E1 Subunit Beta (PDHB), Pyruvate Dehydrogenase E1 Subunit Alpha 1 (PDHA1), ATPase Copper Transporting Alpha (ATP7A), ATPase Copper Transporting Beta (ATP7B), Ferredoxin 1 (FDX1), Glycine Cleavage System Protein H (GCSH), Solute Carrier Family 31 Member 1 (SLC31A1), Dihydrolipoamide Branched Chain Transacylase E2 (DBT), Dihydrolipoamide Dehydrogenase (DLD) and Dihydrolipoamide S-Succinyltransferase (DLST). Induction of cuproptosis could be a potential alternative strategy to eliminate tumor cells and improve survival in HCC patients¹⁰. However, the biological significance of copper homeostasis in HCC has not been fully elucidated.

In our study (Fig. 1), based on the gene expression profiles obtained from the TCGA database and related clinical information, we performed a preliminary analysis of 13 cuproptosis-related genes expressed in HCC and selected liver cancer tissues for experimental validation to screen for the most prognostically significant differentially expressed gene, DLAT, and further explored the potential role of DLAT in HCC. In conclusion, our study suggests that DLAT may be a promising biomarker and target for the prediction of prognosis and development of treatment strategies for HCC.

Results

Expression of the cuproptosis-related gene DLAT is significantly upregulated in HCC

The gene expression data of 424 patients (including 374 tumors and 50 normal) were downloaded from the UCSC Xena database. Differential expression analysis showed that 10 cuproptosis-related genes were differentially expressed between HCC samples and normal samples (Fig. 2A). Univariate COX regression analysis showed that the expression levels of DLAT, LIPT1, PDHA1 and ATP7A were correlated with OS in HCC patients (Fig. 3A). Among them, the differential gene DLAT is the most relevant to the OS of HCC patients ($P=4.1e-5$). Therefore, we selected the gene DLAT for further study. Subsequently, immunohistochemical staining of DLAT protein in 11 HCC tissues was obtained from the HPA database (Fig. 4A), of which 7 HCC tissues showed strong staining, 4 showed medium staining and normal liver tissues showed weak or no staining. Next, we selected multiple datasets in the HCCDB database as a validation cohort to verify the expression level of DLAT in HCC (Fig. 2C). In addition, we performed a pancancer expression analysis of DLAT (Fig. 2B). The results showed that, except for HCC, DLAT was expressed at higher levels in bile duct cancer, esophageal cancer, lung adenocarcinoma, lung squamous cell carcinoma, and gastric adenocarcinoma compared with normal tissue, while it was expressed at lower levels in invasive breast cancer, colon cancer, head and neck squamous cell carcinoma, renal clear cell carcinoma, renal papillary cell carcinoma, prostate adenocarcinoma, rectal adenocarcinoma, melanoma metastasis, and thyroid cancer.

Furthermore, we selected 20 matched HCC tissues and adjacent normal tissues from Affiliated Nantong Hospital 3 of Nantong University as a validation cohort for immunohistochemical staining experiments. Similarly, DLAT was significantly highly expressed in HCC (Fig. 4B). In summary, DLAT expression is significantly upregulated in HCC and is a potential biomarker.

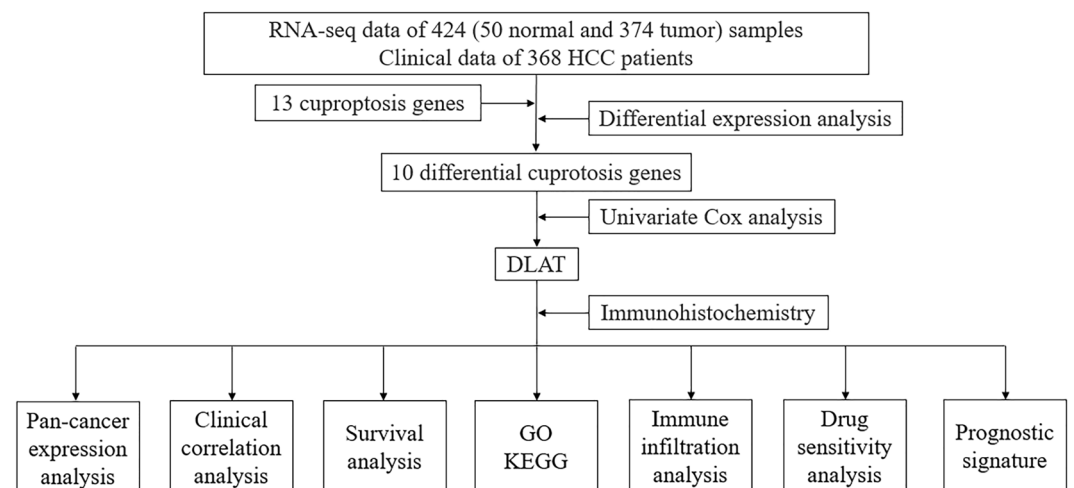


Figure 1. Flow chart of this study.

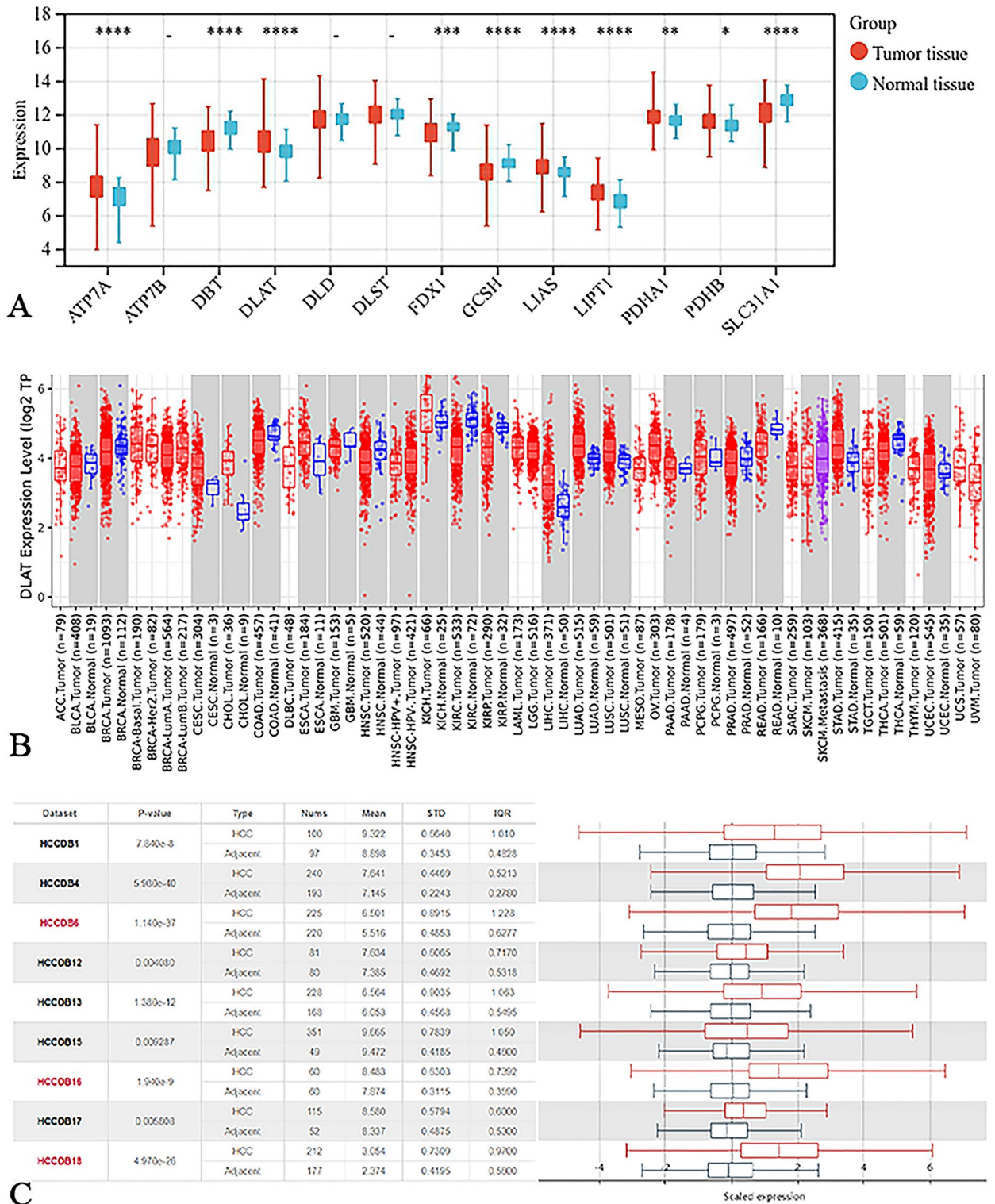


Figure 2. The cuproptosis-related gene DLAT is significantly upregulated in HCC. (A) Expression of 13 cuproptosis-related genes in HCC. (B) Pancancer expression analysis of DLAT between normal and tumor samples according to TIMER. (C) The expression of DLAT in HCC was verified using the HCCDB database. * $P < 0.05$, ** $P < 0.01$, *** $P < 0.001$, **** $P < 0.0001$.

DLAT is related to the prognosis of patients in HCC

According to the median cutoff value of DLAT mRNA expression, 368 HCC patients with clinical and prognostic data were divided into high expression ($n = 134$) and low expression groups ($n = 134$), and survival analysis

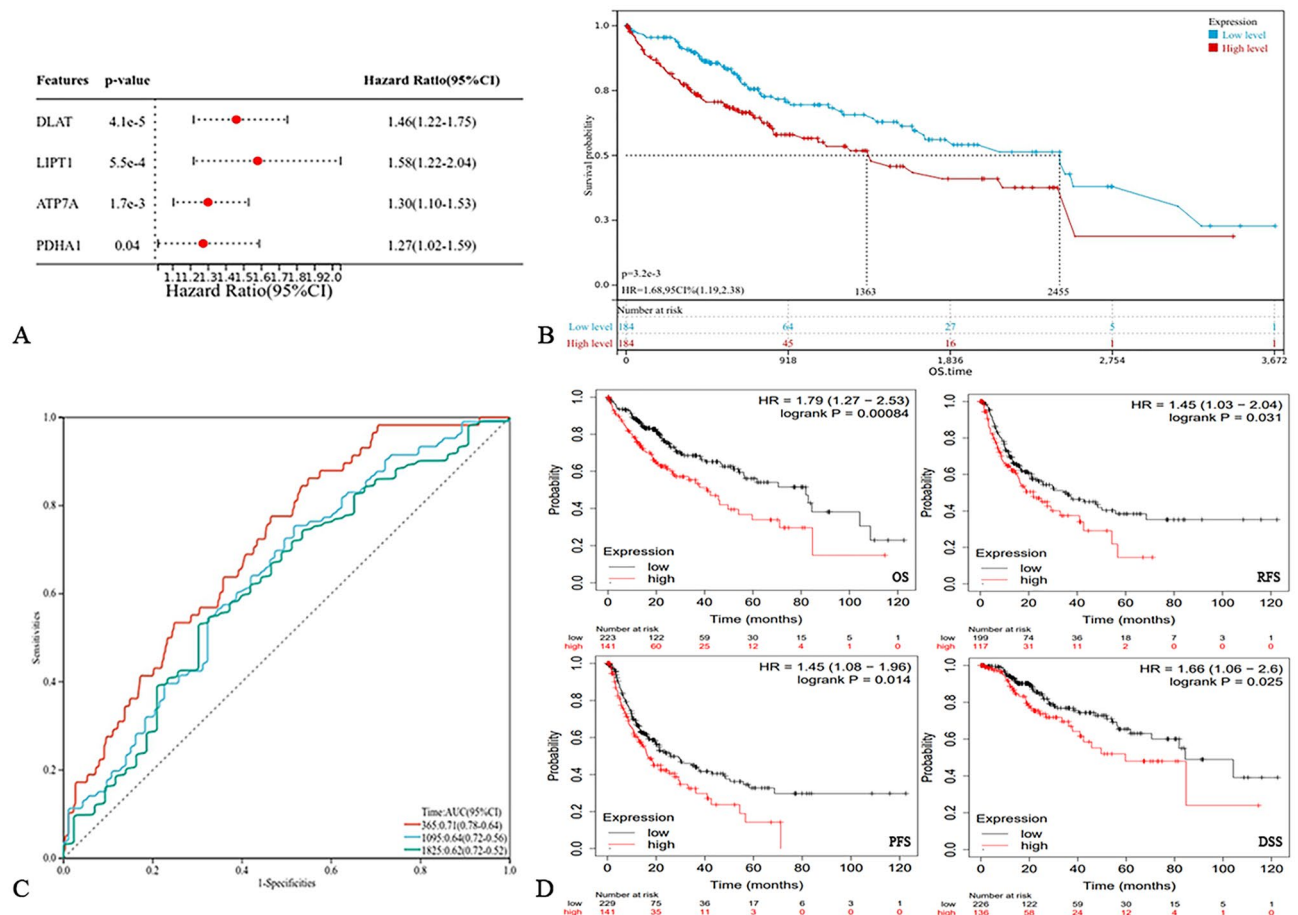


Figure 3. Prognostic value of DLAT in HCC. (A) Four cuproptosis-related genes, DLAT, LIPT1, PDHA1 and ATP7A, were correlated with the prognosis of HCC patients. (B) Kaplan–Meier survival curves for overall survival in HCC patients according to the expression of DLAT. (C) Time dependent receiver operating characteristic curves of the predictive value of DLAT for overall survival. (D) The prognostic value of DLAT in HCC was verified by the KM-ploter database.

was performed. The Kaplan–Meier survival curve shows that the median survival time (MST) was 2455 days in the low expression group and 1363 days in the high expression group, with a significantly longer OS in the low expression group than in the high expression group ($P < 0.05$; Fig. 3B). To further study the independent prognostic value of DLAT in HCC, we performed univariate and multivariate COX regression analyses based on other clinical characteristics of HCC (Table 1). DLAT was an independent risk factor for OS in HCC patients, with Hazard ratios (HRs) of 1.681 (95% CI 1.186–2.383) and 1.689 (95% CI 1.023–2.788), respectively. In summary, HCC patients with high expression of DLAT have a significantly poor prognosis. In addition, we plotted Time-dependent receiver operating characteristic curves (ROCs) to evaluate the predictive value of DLAT for OS in HCC patients (Fig. 3C). The areas under the curve (AUCs) of the DLAT expression groups for OS at 1, 3 and 5 years were 0.71, 0.64, and 0.62, respectively.

We selected the survival data of HCC patients in the KM-ploter database as a validation cohort to verify the prognostic value of DLAT. Similarly, the OS, disease-specific survival (DSS), progression-free survival (PFS) and recurrence-free survival (RFS) of HCC patients with high DLAT expression were significantly shorter than those with low DLAT expression ($P < 0.05$; Fig. 3D). In summary, HCC patients with high DLAT expression have a significantly poor prognosis. DLAT has good prognostic value in HCC.

Correlation between DLAT and other clinical characteristics of HCC

Based on the clinical characteristics of 368 HCC patients, we analyzed the correlation between the DLAT expression level and these clinical characteristics using statistical methods (Table 2). The expression level of DLAT was correlated with tumor T stage. The higher the expression level of DLAT was, the worse the tumor T stage was. In addition, the expression level of DLAT was not significantly correlated with clinical features such as gender, age, histological stage, albumin, total bilirubin, creatinine, and international normalized ratio (INR).

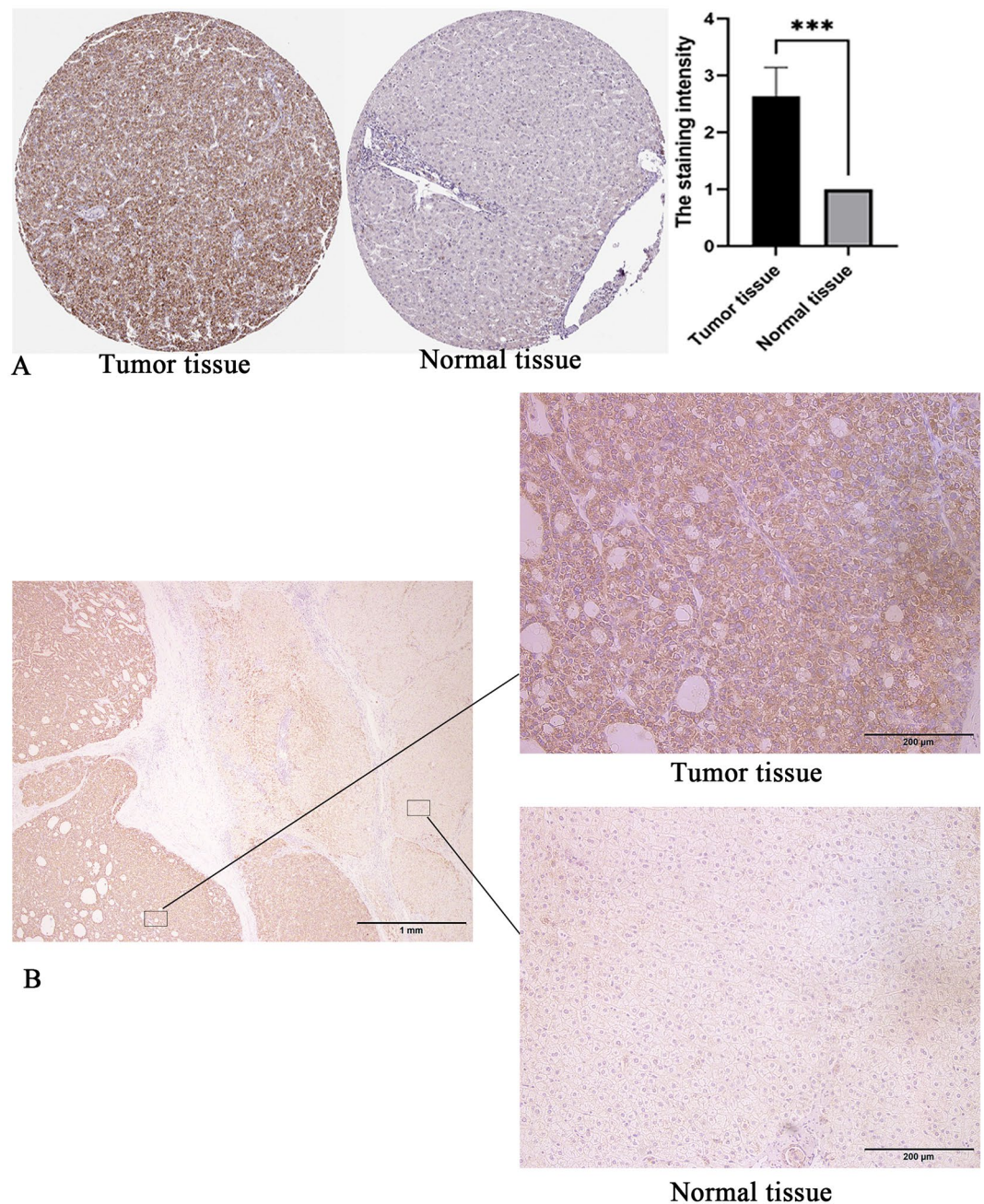


Figure 4. Immunohistochemical staining for DLAT in HCC. (A) The HPA database, $***P < 0.001$. (B) HCC tissues and adjacent normal tissues from Nantong Third Hospital affiliated to Nantong University.

DLAT related gene identification, GeneOntology (GO) and Kyoto Encyclopedia of Genes and Genomes (KEGG) analysis

Based on the LinkedOmics database, 259 genes were associated with DLAT by setting conditions, of which 132 were positively associated and 127 were negatively associated (Fig. 5A; Supplementary Fig. S1). Subsequently, we plotted the protein protein interaction (PPI) network of DLAT and its related genes using the STRING database (Fig. 5B). GO analysis and KEGG pathway analysis were conducted. GO analysis showed that these genes were widely distributed in the nucleus and cytoplasm, mainly enriched in the biosynthesis and metabolism of macromolecules such as proteins in cells, and had molecular functions such as binding to RNA and metal cations in cells and catalytic activity (Fig. 5C). KEGG pathway enrichment analysis showed that these genes were mainly enriched in cell signaling pathways such as cell biological metabolism, tumor progression and immune regulation (Fig. 5D). In addition, the Degree algorithm of the Cytoscape 3.9.1 software CytoNCA plugin was used to obtain 16 related genes with the highest degree of linkage to DLAT, including DIX Domain Containing 1 (DIXDC1), Citrate Synthase (CS), ATP Citrate Lyase (ACLY), NADH: Ubiquinone Oxidoreductase Core Subunit

Factor	Univariable			Multivariable		
	HR	95% CI	P-value	HR	95% CI	P-value
DLAT	1.681	1.186–2.383	0.004	1.689	1.023–2.788	0.040
Sex	1.248	0.876–1.777	0.219			
Age	1.224	0.864–1.733	0.256			
Histological grade	1.115	0.883–1.408	0.362			
Pathologic T	1.672	1.395–2.003	<0.001	1.318	0.996–1.743	0.053
Albumin	0.550	0.323–0.936	0.028	0.407	0.202–0.820	0.012
Total bilirubin	1.533	0.793–2.967	0.204			
Creatinine	0.520	0.345–0.784	0.002	0.947	0.499–1.801	0.869
International normalized ratio	1.602	1.014–2.528	0.043	1.213	0.693–2.123	0.498

Table 1. Univariate and multivariate analyses of OS in patients with liver cancer. *DLAT* dihydrolipoamide S-acetyltransferase, *HR* hazard ratio, *95% CI* 95% confidence interval. *P*-value ≤ 0.05 indicate statistical significance.

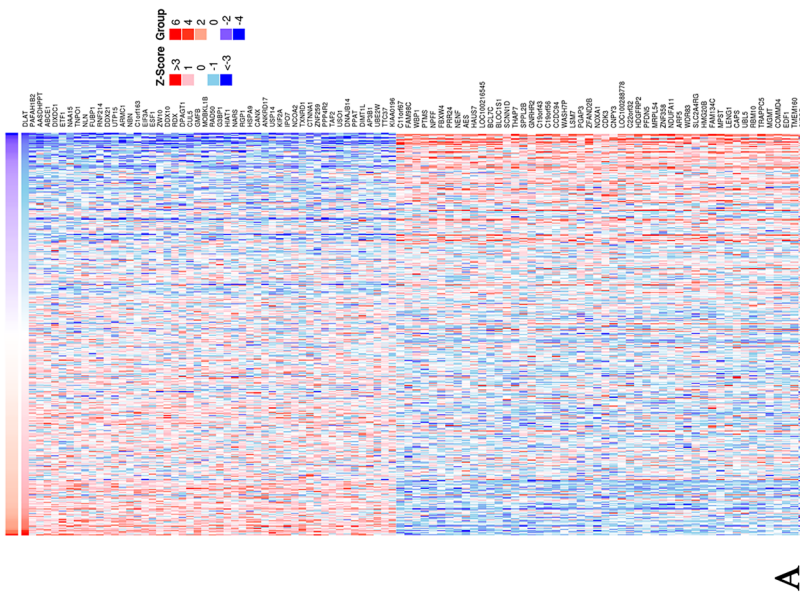
Clinical factor	DLAT expression		P-value
	Low (n = 184)	High (n = 184)	
Sex			
Male	118 (64.1%)	131 (71.2%)	0.147
Female	66 (35.9%)	53 (28.8%)	
Age	64 [54, 68]	60 [51, 69]	0.907
Histological grade			
G1	31 (16.9%)	24 (13.0%)	0.512
G2	81 (44.0%)	95 (51.6%)	
G3	63 (34.2%)	57 (31.0%)	
G4	6 (3.3%)	6 (3.3%)	
Missing	3 (1.6%)	2 (1.1%)	
Pathologic T			
T1	101 (55.0%)	81 (44.0%)	0.047
T2	44 (23.9%)	48 (26.1%)	
T3	33 (17.9%)	45 (24.5%)	
T4	3 (1.6%)	10 (5.4%)	
Missing	3 (1.6%)	0 (0.0%)	
Albumin, g/dL	3.50 [3.50, 3.80]	3.50 [3.50, 3.80]	0.152
Total bilirubin, mg/dL	1.10 [0.76, 3.80]	1.05 [0.70, 2.80]	0.136
Creatinine, mg/dL	1.50 [1.30, 5.89]	1.40 [1.30, 5.60]	0.173
International normalized ratio	1.20 [1.10, 12.00]	1.30 [1.10, 12.00]	0.249

Table 2. Correlation between DLAT and clinical characteristics. *DLAT* dihydrolipoamide S-acetyltransferase. *P*-value ≤ 0.05 indicate statistical significance.

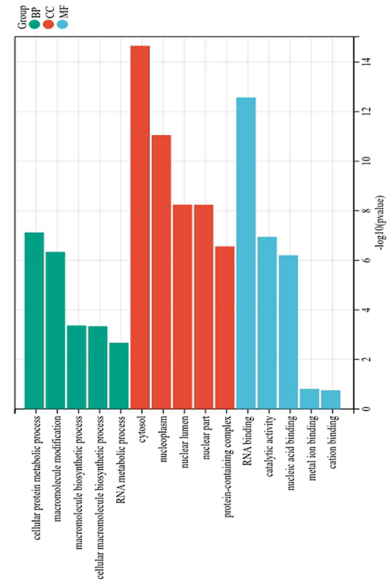
S1 (NDUFS1), Thioredoxin Reductase 1 (TXNRD1), Phosphoglycerate Kinase 1 (PGK1), Ribulose-5-Phosphate-3-Epimerase (RPE), Glutaryl-Prolyl-TRNA Synthetase (EPRS), Argonaute RISC Catalytic Component 2 (AGO2), Succinate Dehydrogenase Complex Subunit D (SDHD), Pyruvate Dehydrogenase Complex Component X (PDHX), Pyruvate Dehydrogenase Phosphatase Catalytic Subunit 2 (PDP2), Sarcolemma Associated Protein (SLMAP), NADH: Ubiquinone Oxidoreductase Subunit B7 (NDUFB7), Glutathione-Disulfide Reductase (GSR), and G Elongation Factor Mitochondrial 1 (GFM1) (Fig. 5E).

Correlation between DLAT and immune infiltration in HCC

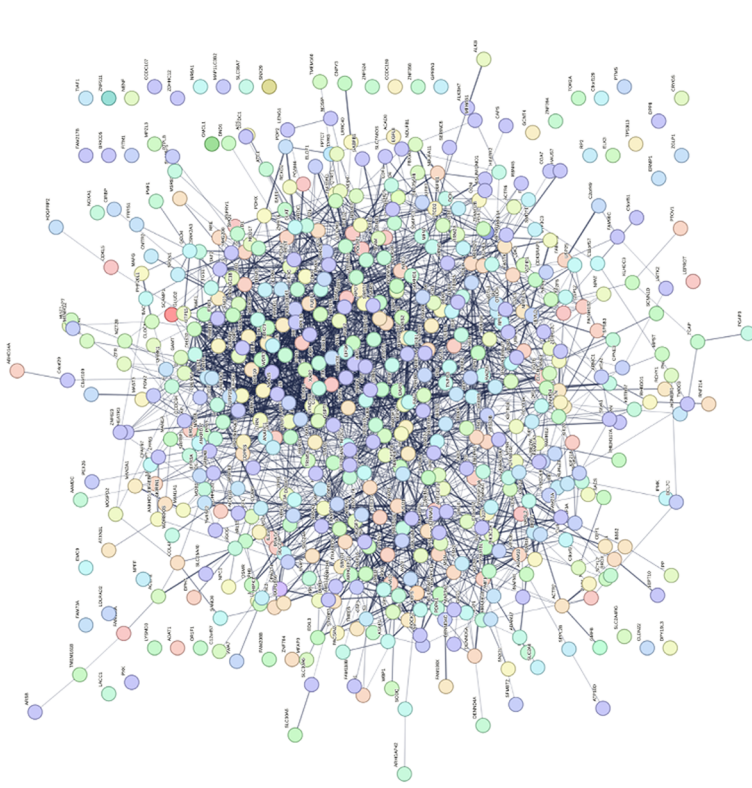
Based on ACLBI and TIMER 2.0 database, we analyzed the correlation between DLAT and the immune cell infiltration levels and immune cell markers. The expression level of DLAT was significantly correlated with various of immune cell infiltration abundances (Fig. 6A–C; Supplementary Figs. S2–S4) and immune cell markers (Fig. 6D). Given the relevance of DLAT to HCC immune infiltration, we also explored the correlation between DLAT and several immune checkpoint-related genes, revealing that DLAT was significantly and positively correlated with CD274, Cytotoxic T-Lymphocyte Associated Protein 4 (CTLA4), Hepatitis A Virus Cellular Receptor 2 (HAVCR2), Programmed Cell Death 1 Ligand 2 (PDCD1LG2) and T Cell Immunoreceptor With Ig And ITIM Domains (TIGIT) (Fig. 6E).



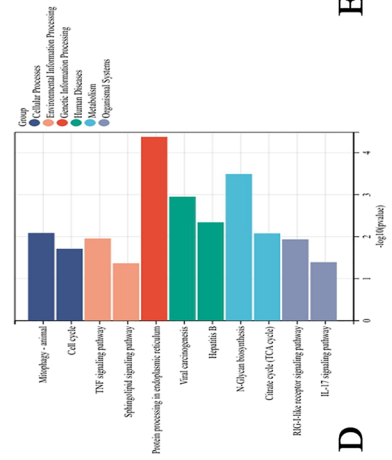
A



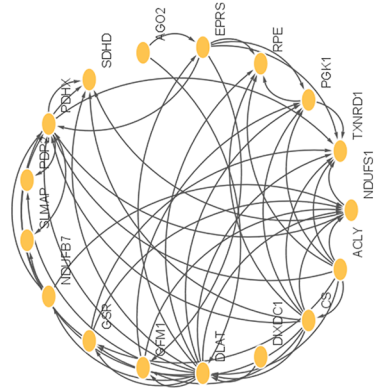
C



B



D



E

Figure 5. Identification of DLAT related genes, pathways and cell functions in HCC. **(A)** The heatmap from the LinkedOmics database showed the top 50 genes positively and negatively correlated with DLAT. **(B)** DLAT related protein interaction network diagram. **(C)** Results from GO analysis. **(D)** Results from KEGG enrichment analysis. **(E)** Based on Cytoscape 3.9.1 software, the genes with the highest link to DLAT were obtained.

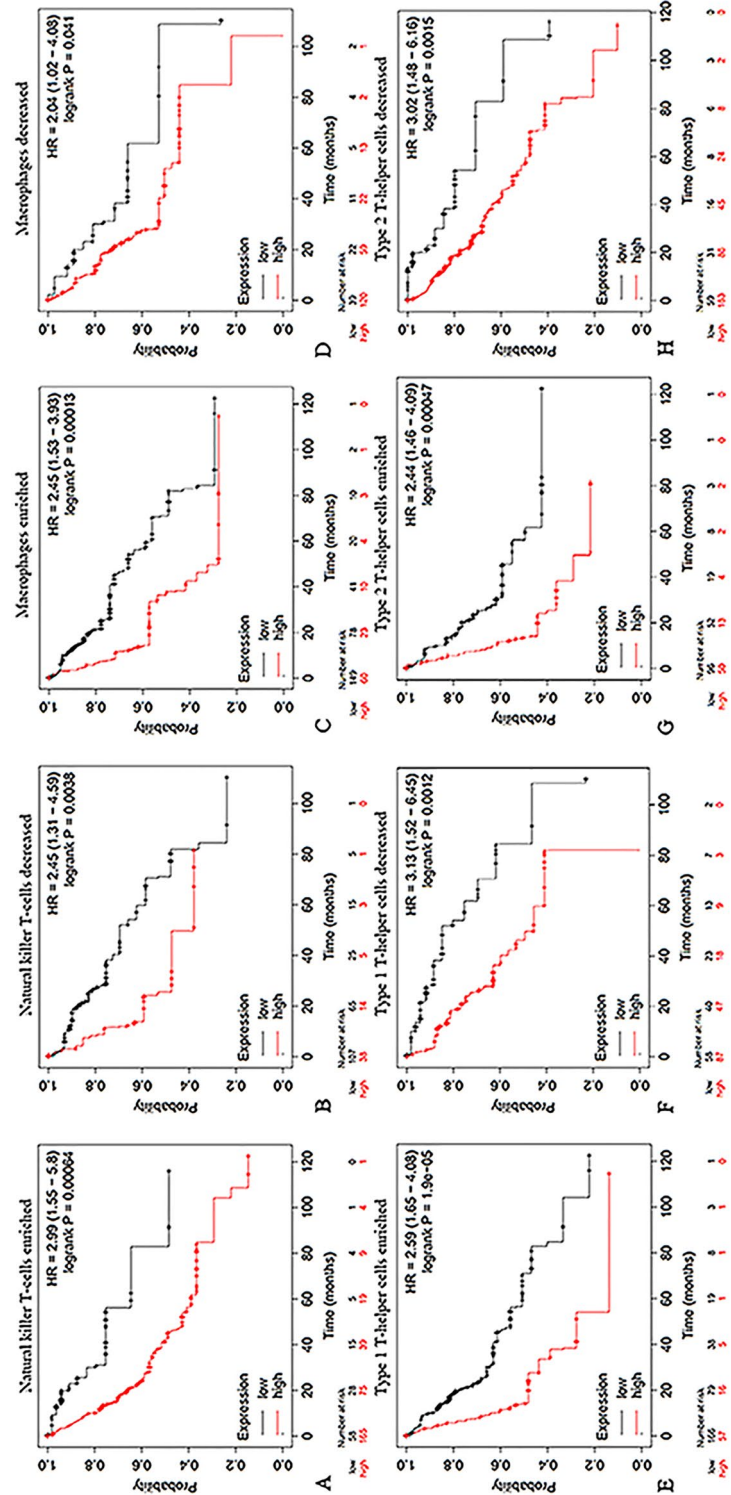


Figure 7. Influence of DLAT expression on the OS of HCC patients with high or low infiltration degrees of immune cells. The impact of DLAT expression on the OS of HCC patients with enriched or decreased infiltration ratios of (A,B) Natural killer T-cells, (C,D) Macrophages, (E,F) Type 1T-helper cells, (G,H) Type 2T-helper cells.

Correlation of DLAT with drug sensitivity

We performed differential analysis of the half maximal inhibitory concentration (IC₅₀) of commonly used drugs (including sorafenib, adriamycin, epirubicin, oxaliplatin, 5-fluorouracil, and cisplatin) between the high and low expression groups of DLAT. The IC₅₀ of sorafenib was significantly lower in the high expression group (Fig. 8A), while the expression of DLAT did not correlate significantly with the IC₅₀ of adriamycin, epirubicin, oxaliplatin, 5-fluorouracil and cisplatin (Fig. 8B–F). Further, survival analysis showed that patients with high DLAT expression (MST = 45.7 months) had a better prognosis than patients with low DLAT expression (MST = 25.6 months) in a group of HCC patients receiving sorafenib (Fig. 8G). This finding suggested that higher DLAT expression in HCC predicts a better response to sorafenib.

Construction of DLAT-related prognosis signature

LASSO Cox regression analysis showed that the four genes had the highest predictive value for OS in liver cancer, and according to lambda (Fig. 9A,B), using the following formula to establish a prognostic signature: Risk score = $(0.075 \times \text{DLAT} + 0.223 \times \text{GSR} + 0.091 \times \text{RPE} + 0.068 \times \text{TXNRD1})$. Using the median risk score as the cut-off value, patients were divided into a high-risk group (n = 184) and low-risk group (n = 183) in the TCGA main cohort.

Principal component analysis (PCA) was performed based on gene expression levels to compare the differences between high-risk and low-risk groups. Prognostic characteristics can clearly classify patients with liver cancer into high-risk and low-risk groups (Fig. 9C). The distribution of the two groups on the PCA diagram is relatively dispersed (Fig. 9D). Kaplan Meier survival analysis showed that patients with higher risk scores were associated with higher risk of death and shorter survival time in the TCGA main cohort (Fig. 9E). We obtained the same results in the ICGC database (Fig. 9F). ROCs evaluated the predictive effect of risk score on OS. The AUCs of 1, 2, and 3 years in the TCGA was 0.77, 0.69, and 0.69 respectively (Fig. 9G), proving that the prognostic signature have good accuracy, specificity and can predict the prognosis of HCC patients.

Discussion

HCC has an insidious onset and lacks typical clinical manifestations in the early stage. Most patients have lost the chance of surgical cure when they are diagnosed. At present, the mortality of HCC is still high, and the 5-year survival rate of patients is less than 20%^{1,4,11}. At the same time, as a highly heterogeneous tumor, HCC is prone to metastasis and recurrence, and the emergence of tumor drug resistance behavior brings great challenges to researchers and clinicians.

Cuproptosis is a new form of cell death. Copper metabolism plays an important role in the development and progression of tumors, and an imbalance of copper homeostasis can induce protein hydrotoxic stress and cell death^{12,13}. Current studies suggest that cuproptosis is largely dependent on the regulation of mitochondrial respiration, in which the tricarboxylic acid cycle (TCA) predominates. Excess copper promotes the clustering of lipid acylated proteins and loss of iron-sulfur cluster proteins by binding the lipid acylated component of TCA enzymes (specifically pyruvate dehydrogenase complex), leading to protein hydrotoxic stress and ultimately to cell death¹⁰.

Cancer metabolism plays an important role in tumor progression and metastasis. In just the last ten years, the significance of metabolic reprogramming has led to its inclusion with the classic hallmarks of cancer¹⁴. The traditional view is that tumor cells prefer to use aerobic glycolysis rather than TCA to obtain energy faster, which is called the Warburg effect¹⁵. The role of TCA in cancer is often neglected. However, in recent years, more and more studies have shown that TCA plays an important role in inflammation, immunity and tumor progression¹⁶. The biochemical reactions in the TCA cycle are catalyzed by many enzymes. Recent findings show that multiple cycle enzymes are either mutated or deregulated in a broad spectrum of cancer, resulting in characteristic metabolic and epigenetic changes that are correlated with disease transformation and progression¹⁷. DLAT, a component E2 of the pyruvate dehydrogenase complex, plays an important role in the linkage between copper toxicity and protein lipid acylation and is crucial gene in the cuproptosis process¹⁸. DLAT plays a role in the progression of many tumors^{19,20}. At present, the expression and function of DLAT in HCC have not been elucidated.

Consistent with the research results of Bai et al.²¹. We have once again verified that DLAT is a prognostic biomarker for HCC patients. Furthermore, correlation analysis showed that DLAT correlated with tumor T-stage, and high levels of DLAT had more advanced T-stage, suggesting that DLAT may have influenced the development of HCC. GO and KEGG pathway enrichment analyses showed that DLAT and its related genes were partially enriched in the anabolism of cellular macromolecules, the TCA cycle and other biomolecular processes. Studies have shown that these biological metabolic processes are specifically involved in HCC formation²². DLAT and its related genes are also enriched in immune response and regulatory pathways such as sphingolipid, IL-17, TNF and RIG-I-like signaling pathways, and the correlation analysis between DLAT and HCC immune cell infiltration indicates that DLAT may also be involved in the immune regulation of HCC. By analyzing the correlation between DLAT and typical immune checkpoints, the expression level of DLAT may affect the efficacy of immunotherapy in HCC patients. It is worth noting that we did not find a significant correlation between DLAT and PD-L1, which is inconsistent with the study of Bai et al.²¹. In addition, a sensitivity analysis of DLAT versus HCC drugs tentatively suggested that HCC with high DLAT expression may benefit more from treatment with sorafenib. Given the good prognostic value of DLAT, we further constructed and evaluated signatures, the prognostic signature had good accuracy, specificity and could predict the prognosis of HCC patients.

Our team has investigated new tumor biomarkers for many years^{6,23}. However, the current research has some limitations. First, the results of the study were mostly based on bioinformatics analyses based on public databases, and we only experimentally validated the expression differences of DLAT. Second, molecular subtypes and treatment information cannot be used for data analysis, potentially impacting the results of bioinformatics

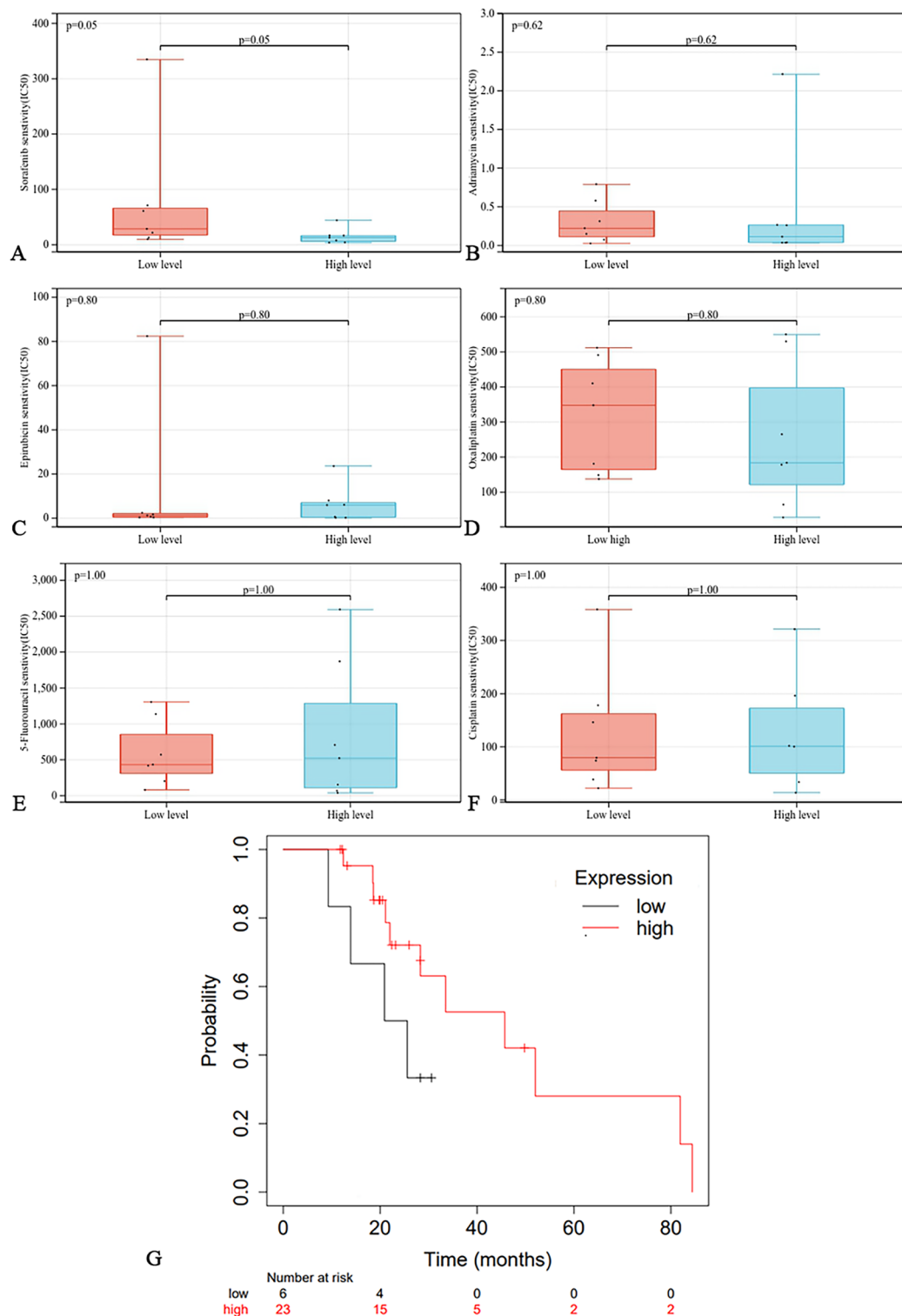


Figure 8. Correlation of DLAT with drug sensitivity. Comparison of the IC50 of antitumor drugs between high and low DLAT expression groups: (A) sorafenib, (B) adriamycin, (C) epirubicin, (D) oxaliplatin, (E) 5-fluorouracil and (F) cisplatin. (G) The correlation between DLAT expression level and prognosis of HCC patients treated with sorafenib.

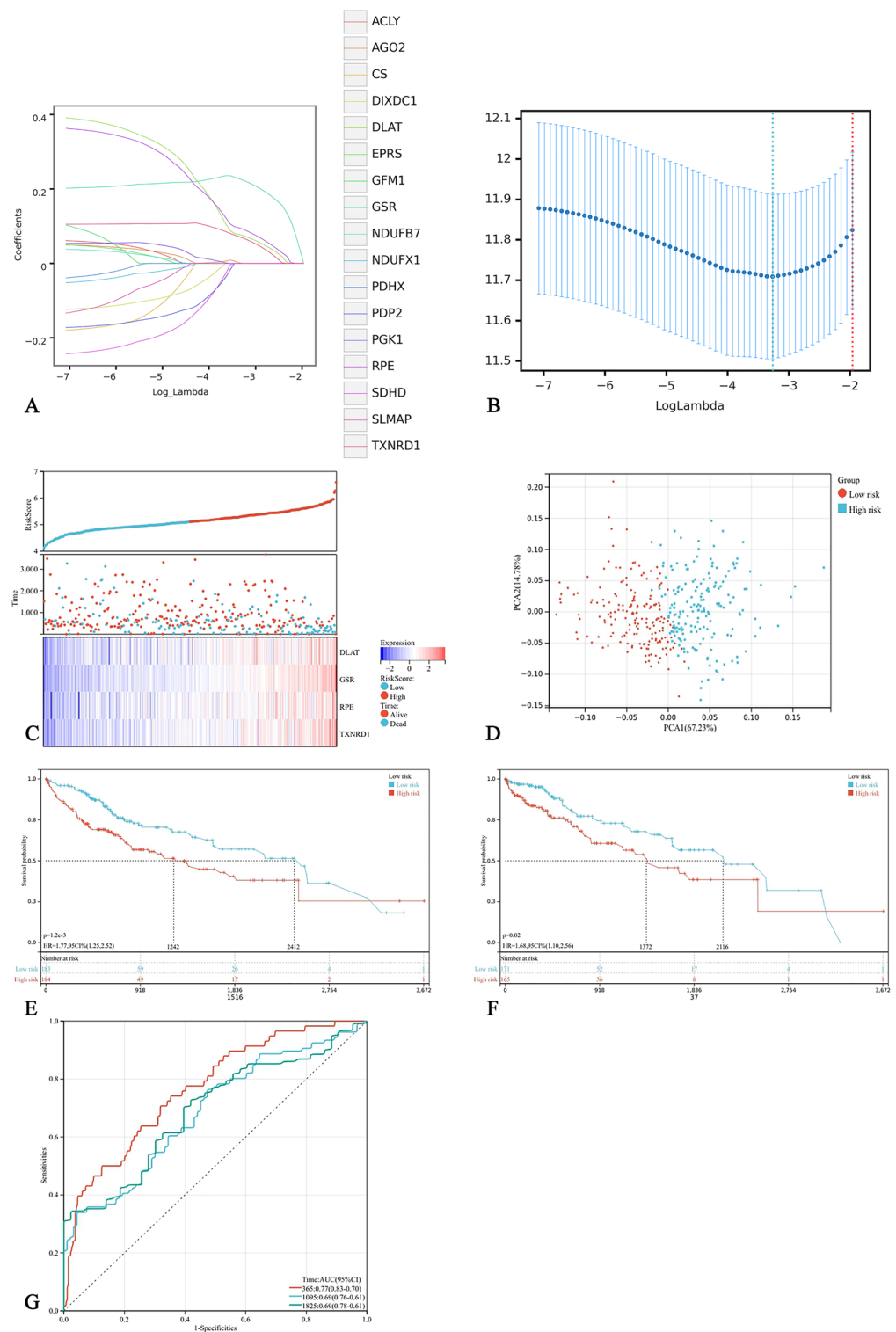


Figure 9. Construction of DLAT-related prognosis signature. **(A)** LASSO coefficient profiles of the DLAT-related genes from the TCGA cohort. **(B)** Lambda value mean square error diagram. The horizontal axis is the logarithm of lambda, the vertical axis is the mean square error, and the two dashed lines are the minimum lambda value and the maximum lambda value within a standard deviation. **(C)** The relationship between different risk scores and patient follow-up time, events, and changes in gene expression. **(D)** PCA analysis. **(E,F)** Kaplan–Meier curve of the prognosis signature in the TCGA cohort and ICGC database. **(G)** ROC analysis for risk signature at 1, 2, and 3 year survival time in the TCGA cohort.

analysis²⁴. In addition, the differential genes LIPT1, PDHA1, and ATP7A are all related to the OS of HCC. More studies are warranted to explore the correlation between these cuproptosis-related genes and HCC, and to construct a multifactor prognostic model to benefit the diagnosis and treatment of HCC in the future.

Conclusion

In summary, based on the validation of DLAT as a prognostic biomarker for hepatocellular carcinoma patients, this study utilized public database data to more comprehensively explore the potential value of DLAT in HCC targeted therapy and immunotherapy. Of course, further experimental exploration is needed. In addition, new prognostic markers have good prognostic value in HCC and can predict the prognosis of HCC patients.

Materials and methods

Patient samples from public databases and validation datasets

The Gene expression quantification data of the transcriptome profiling (HTseq-Counts) of 424 patients in the TCGA-LIHC²⁵ cohort and the clinical and prognostic information of 368 patients were downloaded from the UCSC Xena database²⁶. 20 matched HCC tissue sections and their clinicopathological data from HCC patients undergoing radical surgical resection at Affiliated Nantong Hospital 3 of Nantong University in 2020. All patients were diagnosed according to the HCC guidelines for diagnosis and treatment of the European Association²⁷. The study and experiment were approved by the Ethics Committee of Nantong Third Hospital affiliated to Nantong University and all patients provided their informed consent.

Identification of the most prognostic cuproptosis-related genes in HCC

Differential expression analysis of 13 cuproptosis-related genes between tumor and normal tissues in the TCGA-LIHC cohort was performed by t test, using boxplots to show the results of the analysis. Subsequently, univariate COX regression analysis was used to screen for cuproptosis-related genes with prognostic value. Immunohistochemical staining data of HCC tissues and normal tissues were obtained from the HPA database^{28,29} to verify the differential expression of DLAT in HCC tissues and normal tissues. The screening results were verified by the HCCDB database³⁰. In addition, we explored the pancancer expression levels of DLAT using the TIMER 2.0 database³¹. The Sangerbox Tools platform (<http://www.sangerbox.com/tool>)³² was used for data analysis and visualization.

Immunohistochemistry assay

According to the experimental method of our laboratory⁶, the paraffin sections of HCC tissues were dewaxed with a series of xylene solutions and gradients of ethanol concentrations. The dewaxed tissue slices were dried in a microwave in citrate buffer (pH 6.0) for antigen retrieval. Subsequently, the sections were incubated with 3% H₂O₂ for 15 min to block endogenous peroxidase activity. The sections were incubated overnight at 4 °C with DLAT antibody (13426-1-AP; 1: 500; Proteintech). The next day, we incubated these sections for 30 min at room temperature using horseradish peroxidase-conjugated anti-mouse/rabbit secondary antibody (cat. no. D-3004; Shanghai Changdao Biotechnology Co., Ltd., Shanghai, China). After thorough washing, staining was performed at room temperature for 20 s using 3,3'-diaminobenzene diamine (DAB, Maishin Biologicals, Guangzhou, China). The sections were then stained with hematoxylin and allowed to dry before a coverslip was placed over the surface. Finally, two specialist pathology researchers assessed all stained sections in a blinded manner. The staining intensity was divided into 0–3 grades: 0 (no staining), 1 (weak staining), 2 (medium staining), 3 (strong staining).

Correlation analysis of DLAT and HCC-related clinical characteristics

HCC patients were divided into high and low expression groups according to the median cutoff value of DLAT mRNA expression (Table 3). Based on clinical information from the TCGA-LIHC cohort of 368 HCC patients, we analyzed the correlation between DLAT and HCC-related clinical characteristics. Among them, the enumeration data were tested by chi-square test, the measurement data were tested by independent sample T test, and the nonnormal distribution data were tested by nonparametric rank sum test. $P < 0.05$ was considered statistically significant. SPSS 26.0 software was used for the data analysis of this process.

Prognostic analysis of DLAT in HCC

We evaluated the correlation between DLAT and the OS of HCC patients by plotting Kaplan–Meier survival curves for patients with high and low DLAT expression. Univariate and multivariate COX regression analyses were performed to identify whether DLAT could be used as an independent risk factor for OS in HCC patients. ROCs were constructed to evaluate the predictive value of DLAT for OS in HCC patients. Survival information of HCC patients in the KM-plotter database³³ was used as a validation cohort to verify the prognostic value of DLAT. R packages ‘survival’, ‘timeROC’ and SPSS 26.0 software were used for data analysis and visualization of this process.

Identification of DLAT related genes, pathways and cell functions in HCC

All genes related to DLAT were downloaded from the LinkFinder module of the LinkedOmics database³⁴, and the results were displayed in heatmap from the LinkedOmics database. By setting the conditions $P < 0.05$ and $|\text{Person Correlation}| > 0.3$, the related genes of DLAT were screened. The relevant genomic data were imported into the STRING database (<https://www.string-db.org/>)³⁵ for protein interaction network analysis. Subsequently, GO³⁶ analysis and KEGG³⁷ pathway enrichment analysis were performed to find the molecular mechanism and cell

Clinical factor	No. (%) or median (IQR)
Sex	
Male	119 (32.34%)
Female	249 (67.66%)
Age	61 [52, 69]
Histological grade	
G1	55 (14.95%)
G2	176 (47.83%)
G3	120 (32.61%)
G4	12 (3.26%)
Missing	5 (1.35%)
Pathologic T	
T1	182 (49.46%)
T2	92 (25.00%)
T3	78 (21.20%)
T4	13 (3.53%)
Missing	3 (0.81%)
Albumin, g/dL	3.5 [3.5, 3.8]
Total bilirubin, mg/dL	0.7 [0.5, 1.0]
Creatinine, mg/dL	1.4 [1.2, 1.5]
International normalized ratio	1.2 [1.0, 11.5]
Platelet count, 10 ⁹ /L	150 [130, 150]

Table 3. Clinical characteristics of the included patients.

function enriched by the obtained related genes. For gene set functional enrichment analysis, we used the KEGG rest API (<https://www.kegg.jp/kegg/rest/keggapi.html>) to obtain the latest KEGG Pathway gene annotation, and used the GO annotation of the genes in the R software package org.Hs.eg.db (version 3.1.0). Subsequently, the genes were mapped to two gene sets, and the R software package clusterProfiler (version 3.14.3) was used for enrichment analysis to obtain the results of gene set enrichment. In addition, we used the Degree algorithm of CytoNCA plug-in in Cytoscape 3.9.1 software to obtain 16 related genes with the highest degree of linkage to DLAT. R packages 'org.Hs.eg.db (version 3.1.0)', 'clusterProfiler (version 3.14.3)' were applied in this process.

Correlation analysis of DLAT and HCC immune cell infiltration

The correlation between the DLAT expression level and immune cell infiltration abundance and immune cell markers in HCC was analyzed using the ACLBI (<https://www.aclbi.com/static/index.html#/>) and TIMER 2.0 database. The expression data of seven immune checkpoint-associated genes were obtained by downloading the TCGA-LIHC cohort from the UCSC Xena database, and we analyzed the correlation between DLAT and immune checkpoints and plotted heatmaps. The Sangerbox Tools platform and SPSS 26.0 software were used for data analysis and visualization of this process.

Correlation analysis between DLAT and drug sensitivity of HCC

The GDSC database³⁸ was used to download the IC50 data of commonly used drugs for HCC. The CCLE database³⁹ was used to obtain the expression of DLAT in HCC cells. Subsequently, we analyzed the correlation between the DLAT expression level and IC50 of commonly used drugs for HCC (sorafenib, adriamycin, epirubicin, oxaliplatin, 5-fluorouracil, cisplatin). The 'reshape2', 'ggpubr', 'ggplot2', 'pRRophetic' and 'corrplot' packages of R software were utilized in the procedure.

Prediction signature

Given the good prognostic value of DLAT, we further constructed and evaluated signatures. Where the TCGA cohort is used as a training set and the ICGC data is used as a verification set. "Glmnet" software was used for lasso analysis and the following formula was used for calculation to establish a prognostic risk signature:

$$\sum_{i=1}^n \text{Coef}(\text{Gene}) \times \text{Expr}(\text{Gene})$$

where Coef (gene) is the coefficient of DLAT related genes, and Expr (gene) is the median of gene expression characteristics according to risk scores⁴⁰. K–M and ROC curves were used to test the accuracy of the prediction signature in predicting the prognosis of HCC patients.

Ethics approval and consent to participate

This study was conducted in accordance with the Declaration of Helsinki. It was approved by the Ethics Committee of Affiliated Nantong Hospital 3 of Nantong University. Informed consent was obtained from all patients included in this study.

Data availability

The datasets generated and analyzed during the current study are available from the corresponding author on reasonable request. The raw data could also be obtained from online databases including the UCSC Xena (<https://xena.ucsc.edu/>), HPA database (<https://www.proteinatlas.org/>), HCCDB (<http://lifeome.net/database/hccdb/search.html>), TIMER 2.0 database (<http://timer.comp-genomics.org>), KM-plotter database (<http://kmplot.com/analysis/>), LinkedOmic database (<http://www.linkedomics.org/login.php>), GDSC database (<https://www.cancerrxgene.org/>), CCLE database (<https://sites.broadinstitute.org/ccle>), ICGC database (<https://dcc.icgc.org/>) without any restrictions.

Received: 17 April 2023; Accepted: 28 September 2023

Published online: 12 October 2023

References

1. Yang, J. D. *et al.* A global view of hepatocellular carcinoma: Trends, risk, prevention and management. *Nat. Rev. Gastroenterol. Hepatol.* **16**(10), 589–604 (2019).
2. Couri, T. & Pillai, A. Goals and targets for personalized therapy for HCC. *Hep. Intl.* **13**(2), 125–137 (2019).
3. Llovet, J. M. *et al.* Hepatocellular carcinoma. *Nat. Rev. Dis. Primers* **7**(1), 6 (2021).
4. Sung, H. *et al.* Global cancer statistics 2020: GLOBOCAN estimates of incidence and mortality worldwide for 36 cancers in 185 countries. *CA Cancer J. Clin.* **71**(3), 209–249 (2021).
5. Qu, X., Yeung, C., Coleman, I., Nelson, P. S. & Fang, M. Comparison of four next generation sequencing platforms for fusion detection: Oncomine by ThermoFisher, AmpliSeq by illumina, FusionPlex by ArcherDX, and QIaseq by QIAGEN. *Cancer Genet.* **243**, 11–18 (2020).
6. Zhang, P. *et al.* Expression and function of myelin expression factor 2 in hepatocellular carcinoma. *BMC Gastroenterol.* **23**(1), 20 (2023).
7. Tang, R. *et al.* Ferroptosis, necroptosis, and pyroptosis in anticancer immunity. *J. Hematol. Oncol.* **13**(1), 110 (2020).
8. Su, Z., Yang, Z., Xu, Y., Chen, Y. & Yu, Q. Apoptosis, autophagy, necroptosis, and cancer metastasis. *Mol. Cancer* **14**, 48 (2015).
9. Chen, L., Min, J. & Wang, F. Copper homeostasis and cuproptosis in health and disease. *Signal Transduct. Target. Ther.* **7**(1), 378 (2022).
10. Tsvetkov, P. *et al.* Copper induces cell death by targeting lipoylated TCA cycle proteins. *Science (New York, NY)* **375**(6586), 1254–1261 (2022).
11. Zeng, H. *et al.* Changing cancer survival in China during 2003–15: A pooled analysis of 17 population-based cancer registries. *Lancet Global Health* **6**(5), e555–e567 (2018).
12. Aggett, P. J. An overview of the metabolism of copper. *Eur. J. Med. Res.* **4**(6), 214–216 (1999).
13. Scheiber, I., Dringen, R. & Mercer, J. F. Copper: Effects of deficiency and overload. *Metal Ions Life Sci.* **13**, 359–387 (2013).
14. Hanahan, D. & Weinberg, R. A. Hallmarks of cancer: The next generation. *Cell* **144**(5), 646–674 (2011).
15. Warburg, O., Wind, F. & Negelein, E. The metabolism of tumors in the body. *J. Gen. Physiol.* **8**(6), 519–530 (1927).
16. Sajjani, K., Islam, F., Smith, R. A., Gopalan, V. & Lam, A. K. Genetic alterations in Krebs cycle and its impact on cancer pathogenesis. *Biochimie* **135**, 164–172 (2017).
17. Anderson, N. M., Mucka, P., Kern, J. G. & Feng, H. The emerging role and targetability of the TCA cycle in cancer metabolism. *Protein Cell* **9**(2), 216–237 (2018).
18. Vijaykrishnan, S. *et al.* Solution structure and characterisation of the human pyruvate dehydrogenase complex core assembly. *J. Mol. Biol.* **399**(1), 71–93 (2010).
19. Chen, Q. *et al.* PM25 promotes NSCLC carcinogenesis through translationally and transcriptionally activating DLAT-mediated glycolysis reprogramming. *J. Exp. Clin. Cancer Res.* **41**(1), 229 (2022).
20. Goh, W. Q., Ow, G. S., Kuznetsov, V. A., Chong, S. & Lim, Y. P. DLAT subunit of the pyruvate dehydrogenase complex is upregulated in gastric cancer-implications in cancer therapy. *Am. J. Transl. Res.* **7**(6), 1140–1151 (2015).
21. Bai, W. D. *et al.* A novel cuproptosis-related signature identified DLAT as a prognostic biomarker for hepatocellular carcinoma patients. *World J. Oncol.* **13**(5), 299–310 (2022).
22. Ferrarini, A. *et al.* Metabolomic analysis of liver tissues for characterization of hepatocellular carcinoma. *J. Proteome Res.* **18**(8), 3067–3076 (2019).
23. Ju, L. L. *et al.* Effect of NDC80 in human hepatocellular carcinoma. *World J. Gastroenterol.* **23**(20), 3675–3683 (2017).
24. Li, L., Li, L. & Sun, Q. High expression of cuproptosis-related SLC31A1 gene in relation to unfavorable outcome and deregulated immune cell infiltration in breast cancer: An analysis based on public databases. *BMC Bioinf.* **23**(1), 350 (2022).
25. Comprehensive and Integrative Genomic Characterization of Hepatocellular Carcinoma. *Cell* **169**(7), 1327–1341.e1323 (2017).
26. Goldman, M. J. *et al.* Visualizing and interpreting cancer genomics data via the Xena platform. *Nat. Biotechnol.* **38**(6), 675–678 (2020).
27. EASL-EORTC clinical practice guidelines. management of hepatocellular carcinoma. *J. Hepatol.* **56**(4), 908–943 (2012).
28. Uhlén, M. *et al.* Proteomics: Tissue-based map of the human proteome. *Science (New York, NY)* **347**(6220), 1260419 (2015).
29. Uhlen, M. *et al.* Towards a knowledge-based Human Protein Atlas. *Nat. Biotechnol.* **28**(12), 1248–1250 (2010).
30. Lian, Q. *et al.* HCCDB: A database of hepatocellular carcinoma expression atlas. *Genom. Proteomics, Bioinf.* **16**(4), 269–275 (2018).
31. Li, T. *et al.* TIMER: A web server for comprehensive analysis of tumor-infiltrating immune cells. *Cancer Res.* **77**(21), e108–e110 (2017).
32. Shen, W. *et al.* Sangerbox: A comprehensive, interaction-friendly clinical bioinformatics analysis platform. *iMeta* **1**(3), e36 (2022).
33. Lánckzy, A. & Györfy, B. Web-Based Survival Analysis Tool Tailored for Medical Research (KMplot): Development and Implementation. *J. Med. Internet Res.* **23**(7), e27633 (2021).
34. Vasaikar, S. V., Straub, P., Wang, J. & Zhang, B. LinkedOmics: Analyzing multi-omics data within and across 32 cancer types. *Nucleic Acids Res.* **46**(D1), D956–d963 (2018).
35. Szklarczyk, D. *et al.* STRING v10: Protein–protein interaction networks, integrated over the tree of life. *Nucleic Acids Res.* **43**, D447–D452 (2015).
36. Ashburner, M. *et al.* Gene ontology: Tool for the unification of biology The Gene Ontology Consortium. *Nat. Genet.* **25**(1), 25–29 (2000).
37. Kanehisa, M. & Goto, S. KEGG: Kyoto encyclopedia of genes and genomes. *Nucleic Acids Res.* **28**(1), 27–30 (2000).

38. Yang, W. *et al.* Genomics of Drug Sensitivity in Cancer (GDSC): A resource for therapeutic biomarker discovery in cancer cells. *Nucleic Acids Res.* **41**, D955–D961 (2013).
39. Barretina, J. *et al.* The Cancer Cell Line Encyclopedia enables predictive modelling of anticancer drug sensitivity. *Nature* **483**(7391), 603–607 (2012).
40. Zhang, Q. *et al.* A prognostic signature of cuproptosis and TCA-related genes for hepatocellular carcinoma. *Front. Oncol.* **12**, 1040736 (2022).

Acknowledgements

Thanks to the technical support provided by experts in the Department of Pathology, Affiliated Nantong Hospital 3 of Nantong University.

Author contributions

Study concept and design: Z.P., C.L. and C.W.H. Experiment and data acquisition: Z.J.H., Y.L.X. and W.H.X. Analysis and interpretation of data: Z.P. and J.L.L. Statistical analysis: Z.J.H. and W.F. Drafting of the manuscript: Z.P. and Z.J.H. Funding: W.H.X. and Y.L.X. All authors contributed to the article and approved the submitted version.

Funding

This study was supported by the Nantong Science and Technology Bureau (Grant/Award Numbers: JCZ2022080) and the Nantong Municipal Health Commission (Grant/Award Numbers: QA20210039, QN2022041).

Competing interests

The authors declare no competing interests.

Additional information

Supplementary Information The online version contains supplementary material available at <https://doi.org/10.1038/s41598-023-43835-y>.

Correspondence and requests for materials should be addressed to L.C. or W.-H.C.

Reprints and permissions information is available at www.nature.com/reprints.

Publisher's note Springer Nature remains neutral with regard to jurisdictional claims in published maps and institutional affiliations.



Open Access This article is licensed under a Creative Commons Attribution 4.0 International License, which permits use, sharing, adaptation, distribution and reproduction in any medium or format, as long as you give appropriate credit to the original author(s) and the source, provide a link to the Creative Commons licence, and indicate if changes were made. The images or other third party material in this article are included in the article's Creative Commons licence, unless indicated otherwise in a credit line to the material. If material is not included in the article's Creative Commons licence and your intended use is not permitted by statutory regulation or exceeds the permitted use, you will need to obtain permission directly from the copyright holder. To view a copy of this licence, visit <http://creativecommons.org/licenses/by/4.0/>.

© The Author(s) 2023